

# Batteries & Supercaps

Supporting Information

## **SiCN Ceramics as Electrode Materials for Sodium/Sodium Ion Cells – Insights from $^{23}\text{Na}$ In-Situ Solid-State NMR**

Edina Šić, Marco Melzi d'Eril, Konstantin Schutjajew, Magdalena J. Graczyk-Zajac, Hergen Breitzke, Ralf Riedel, Martin Oschatz, Torsten Gutmann,\* and Gerd Buntkowsky\*

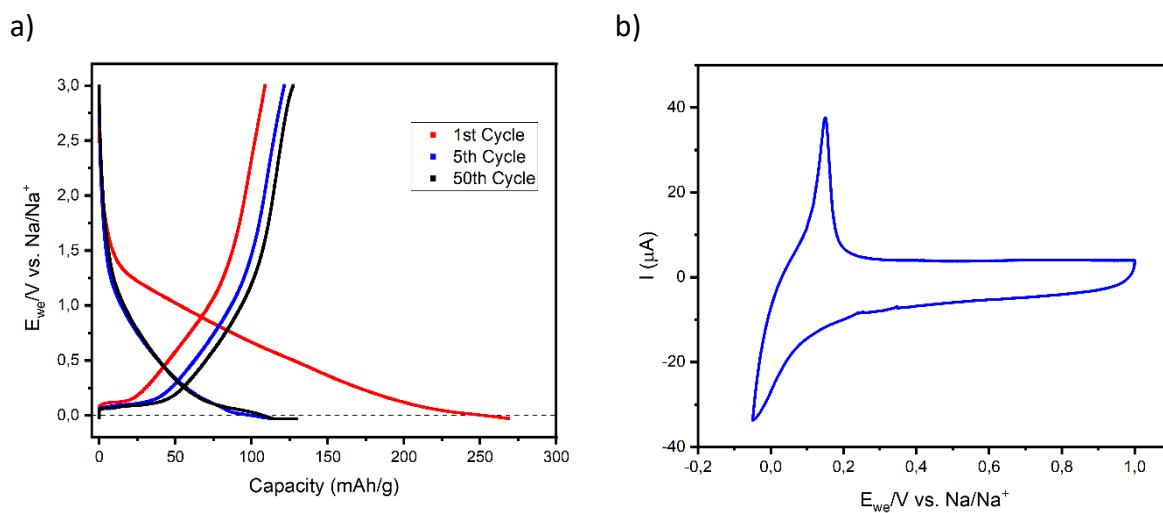


Figure S1: a) Galvanostatic charge/discharge curves of the PDC material during the 1st, 5th and 50th cycle obtained at a mass specific current of  $37.2 \text{ mA g}^{-1}$ . b) Cyclic voltammogram of the PDC material obtained in the voltage range between 1 to  $-0.05 \text{ V vs. Na/Na}^+$  with a rate of  $20 \text{ } \mu\text{V/s}$ .

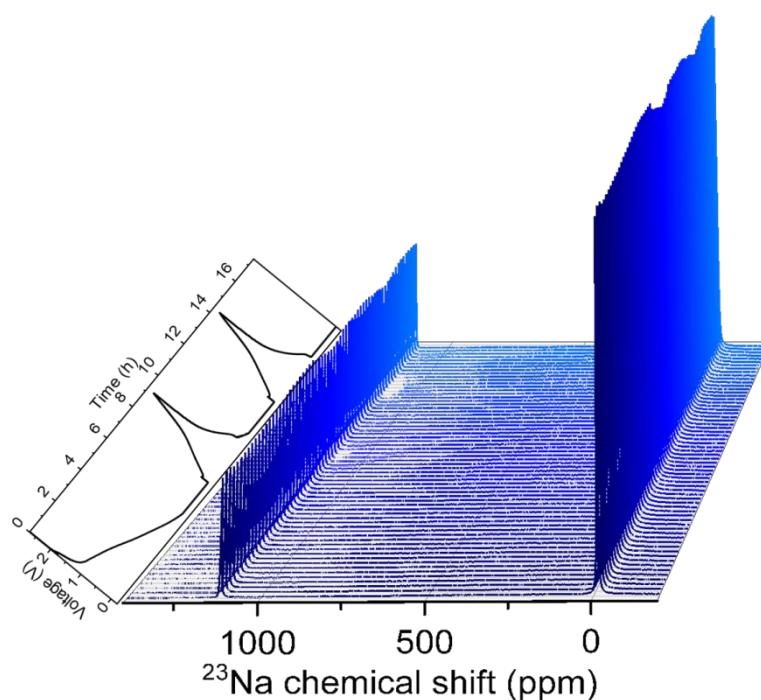


Figure S2:  $^{23}\text{Na}$  *in-situ* NMR spectra for the  $\text{Na}|\text{NaPF}_6|\text{SiCN}$  electrochemical cell. The electrochemical cycling was conducted in the voltage window of  $-0.03$  to  $2.5 \text{ V}$  applying a current of  $\pm 75 \text{ } \mu\text{A}$  for  $16.56 \text{ h}$ . A 3D enlarged view of the metal and electrolyte region is presented in the main manuscript in Figure 1.

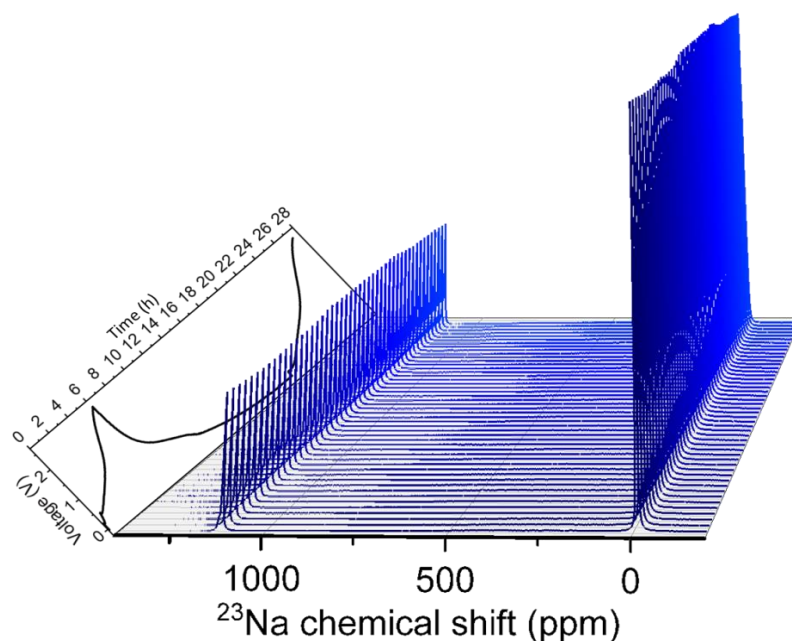


Figure S3:  $^{23}\text{Na}$  *in-situ* NMR spectra of the  $\text{Na}|\text{NaPF}_6|\text{SiCN}$  cell obtained when galvanostatic cycling was performed with a current of  $\pm 20 \mu\text{A}$  at a rate of  $\text{C}/30$  corresponding to the graphite specific capacity of  $372 \text{ mAhg}^{-1}$ .

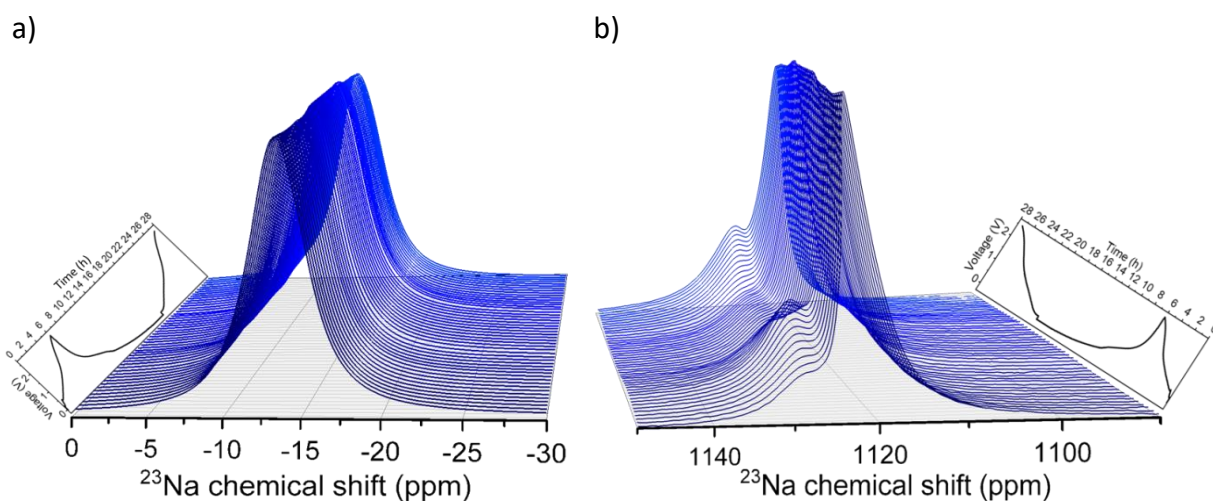


Figure S4: Enlarged 3D view of the  $^{23}\text{Na}$  *in-situ* NMR spectra presented in Figure S3 for a) the electrolyte region (0 to -30 ppm) and b) the metal region (1150 to 1090 ppm). An increase respectively decrease of the shoulder signal at 1128 ppm during the desodiation and sodiation is visible.

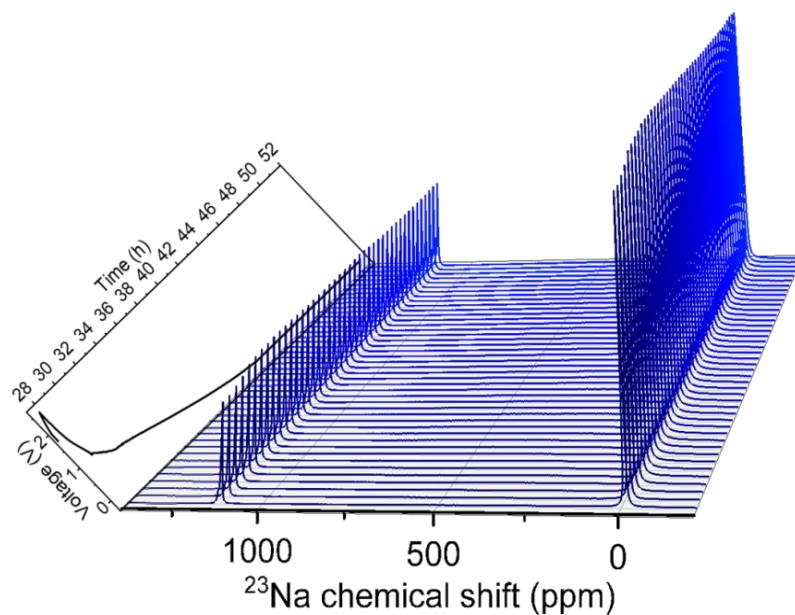
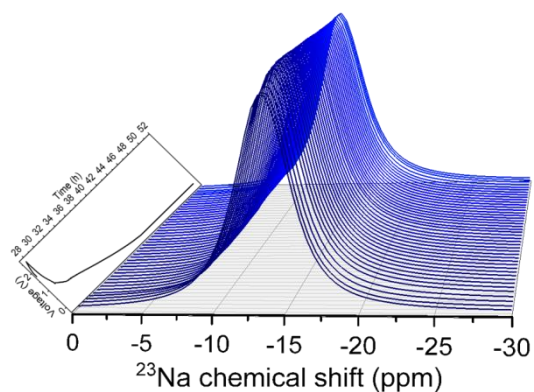


Figure S5:  $^{23}\text{Na}$  *in-situ* NMR spectra of the Na|NaPF<sub>6</sub>|SiCN cell obtained when galvanostatic performance was carried out with a current of  $\pm 20 \mu\text{A}$  at a rate of C/30 corresponding to the graphite specific capacity of  $372 \text{ mAhg}^{-1}$ . When the voltage minimum has been achieved, the cell was held at  $-0.03 \text{ V}$  for around 10 hrs.

a)



b)

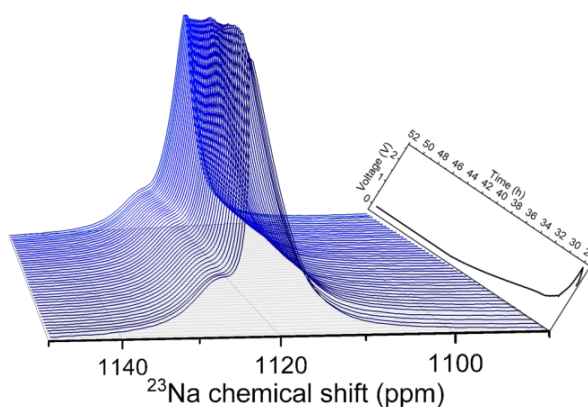
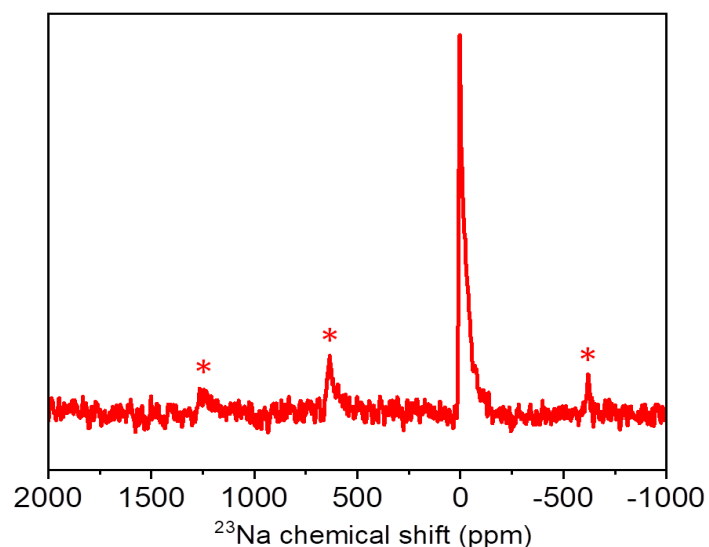
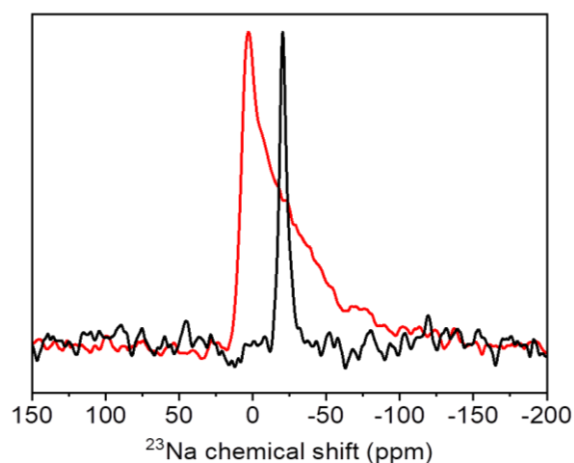


Figure S6: Enlarged 3D view of the  $^{23}\text{Na}$  *in-situ* NMR spectra presented in Figure S5 for a) the electrolyte region (0 to  $-30 \text{ ppm}$ ) and b) the metal region (1150 to  $1090 \text{ ppm}$ ). Along this performance, no significant changes were found in the  $^{23}\text{Na}$  *in-situ* NMR spectra.

a)



b)



c)

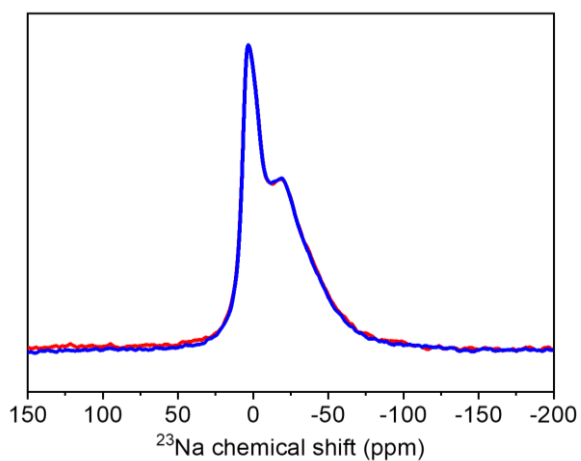
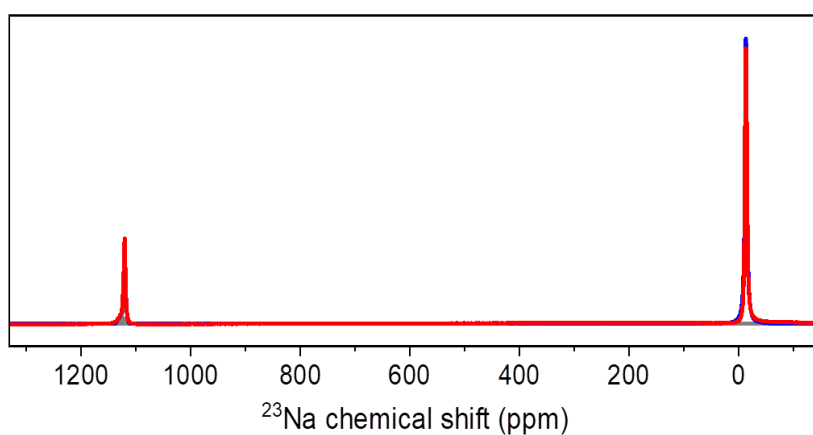
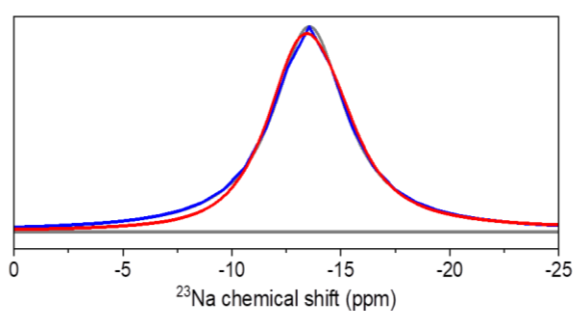


Figure S7: a)  $^{23}\text{Na}$  *ex-situ* MAS NMR spectrum of the cycled SiCN material. The spectrum was recorded at 7 T at a spinning rate of 50 kHz with an offset of 200 ppm employing the Hahn-echo sequence. Note: Spinning sidebands are marked with asterisks. b) Zoom in of spectrum (a) (red spectrum) and of the spectrum of pristine SiCN material wetted with the electrolyte solution (black spectrum). Note: Both spectra were measured with the same acquisition parameters and are normalized to their maximum height. c) Comparison of the spectra of the cycled SiCN material recorded at 7 T at a spinning rate of 50 kHz with single pulse excitation employing short flip angles of 0.1 and 0.2  $\mu\text{s}$  (blue and red spectra) and 81920 respectively 20480 scans. Note that the spectrum measured with a flip angle of 0.1  $\mu\text{s}$  is scaled by a factor of 1.65 to ease the comparison.

a)



b)



c)

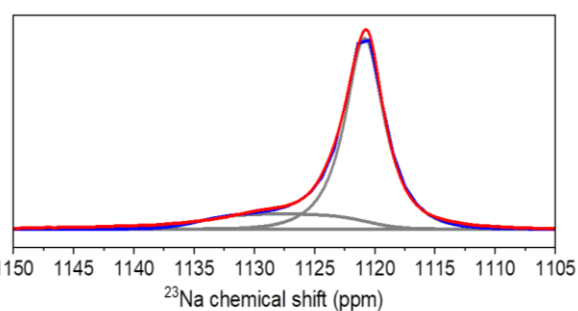


Figure S8: a) An example for the performed deconvolution of the  $^{23}\text{Na}$  *in-situ* NMR spectra by three Gaussian/Lorentzian lines. The experimental spectrum is illustrated as red curve and the cumulative fit peak is displayed as blue curve. Enlarged view of the  $^{23}\text{Na}$  *in-situ* NMR spectrum for b) the electrolyte region (0 to -25 ppm), and c) the metal region including the shoulder structure (1150 to 1105 ppm).

Table S1: Fit data for the  $^{23}\text{Na}$  *in-situ* NMR spectrum shown in Figure S7.

Parameter	Chemical shift (ppm)	FWHM (ppm)	Rel. Area (%)
Fit 1	-13.55	4.00	78.83
Fit 2	1120.84	3.82	17.25
Fit 3	1127.68	13.96	3.92

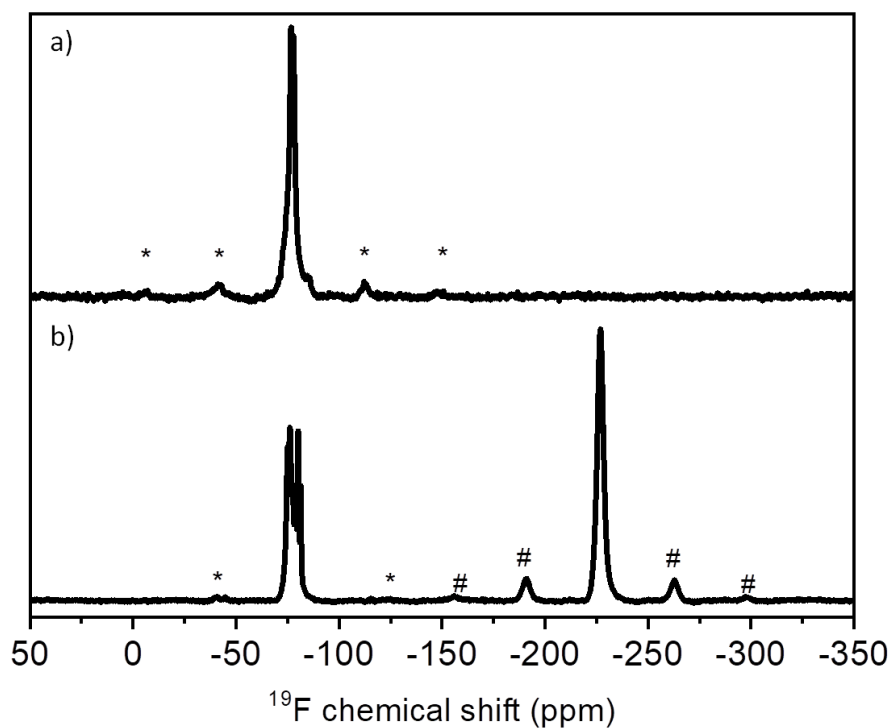


Figure S9:  $^{19}\text{F}$  *ex-situ* MAS NMR spectra of a) the wetted SiCN with  $\text{NaPF}_6$  and b) the cycled SiCN material. Spectra were recorded at 14.1 T at a spinning frequency of 20 kHz.

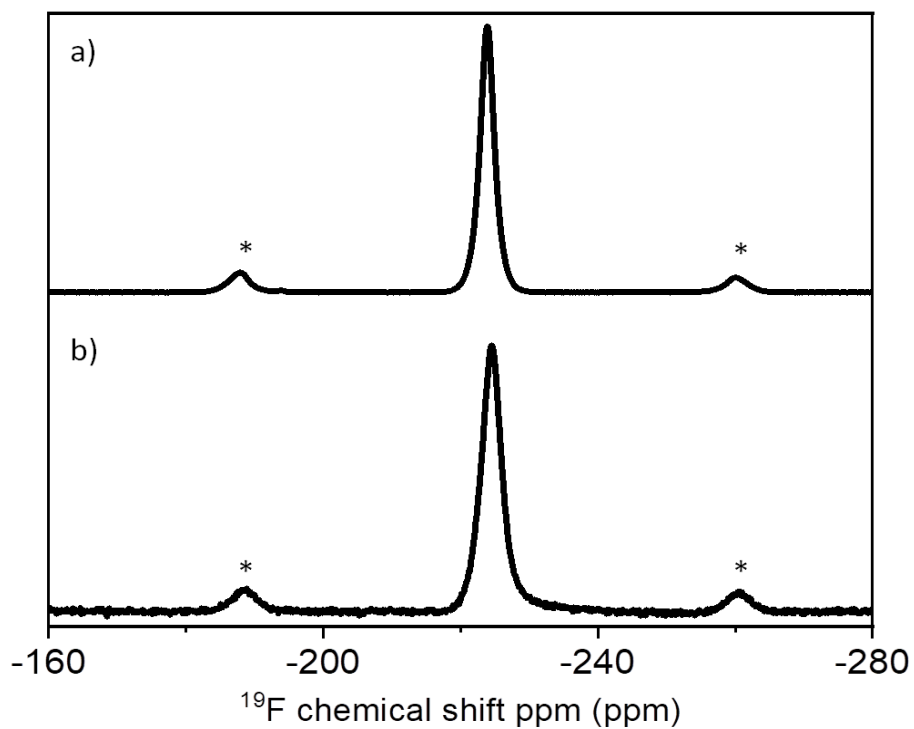


Figure S10: Enlarged view of the  $^{19}\text{F}$  *ex-situ* MAS NMR spectra of a) NaF and b) cycled SiCN shown in S9.

The  $^{19}\text{F}$  *ex-situ* MAS NMR spectra were acquired on a 600 MHz Bruker Avance III HD spectrometer at 14.1 T corresponding to a frequency of 564.68 MHz for  $^{19}\text{F}$ . The measurements were performed using a 1.3 mm MAS rotor at a spinning frequency of 20 kHz and applying single pulse excitation. For the recording of the  $^{19}\text{F}$  spectra a pulse length of 2.1  $\mu\text{s}$  and a recycle delay of 3 s were set accumulating 80 scans. The  $^{19}\text{F}$  chemical shift was referenced relative to  $\text{CFCl}_3$  using the signal of the polytetrafluorethylene (PTFE) at -122.7 ppm as external reference.